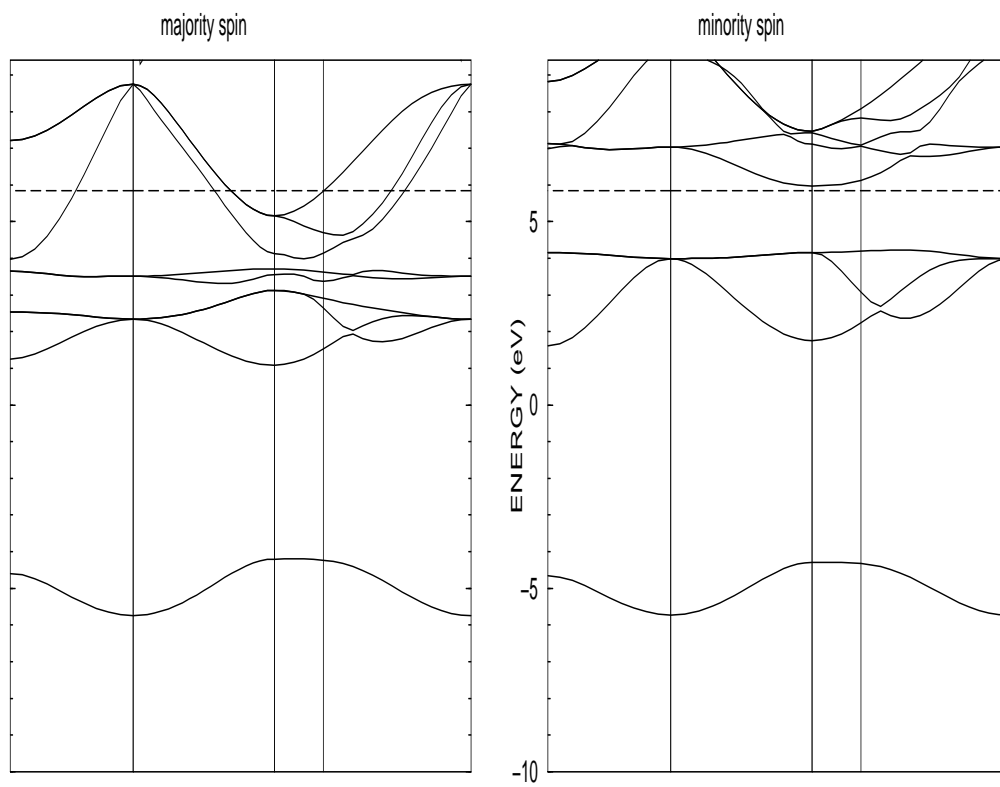


Fig. 1
Reference number of manuscript: A-III.2

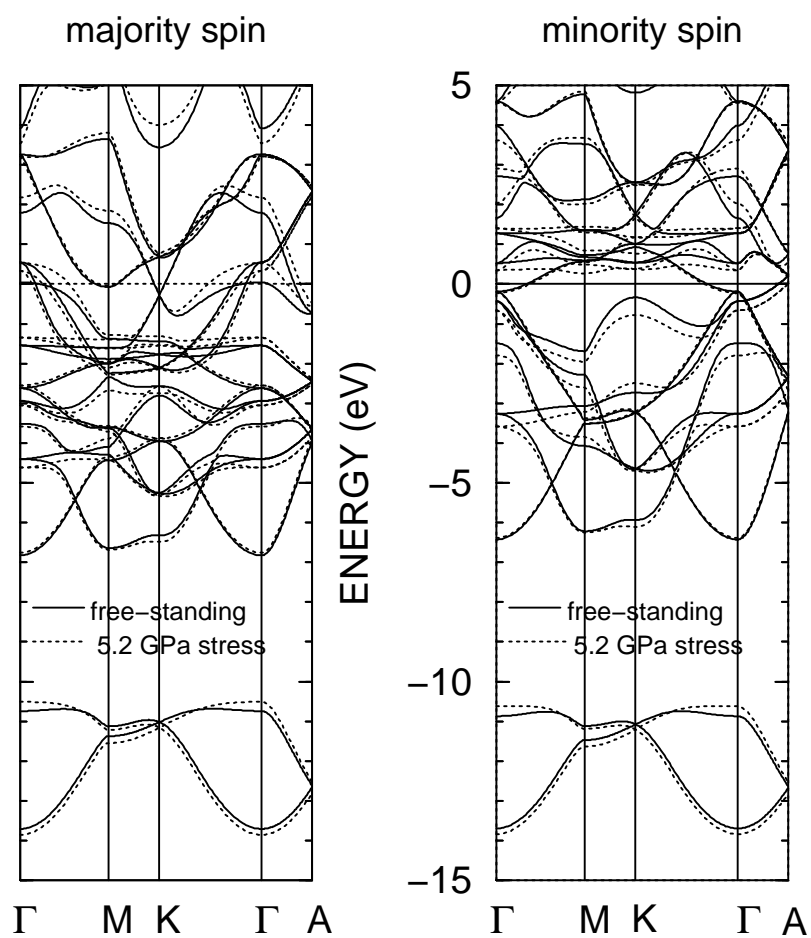
Reference number of manuscript: A-III.2

Fig. 2



Reference number of manuscript: A-III.2

Fig. 3



Reference number of manuscript: A-III.2

Fig. 4

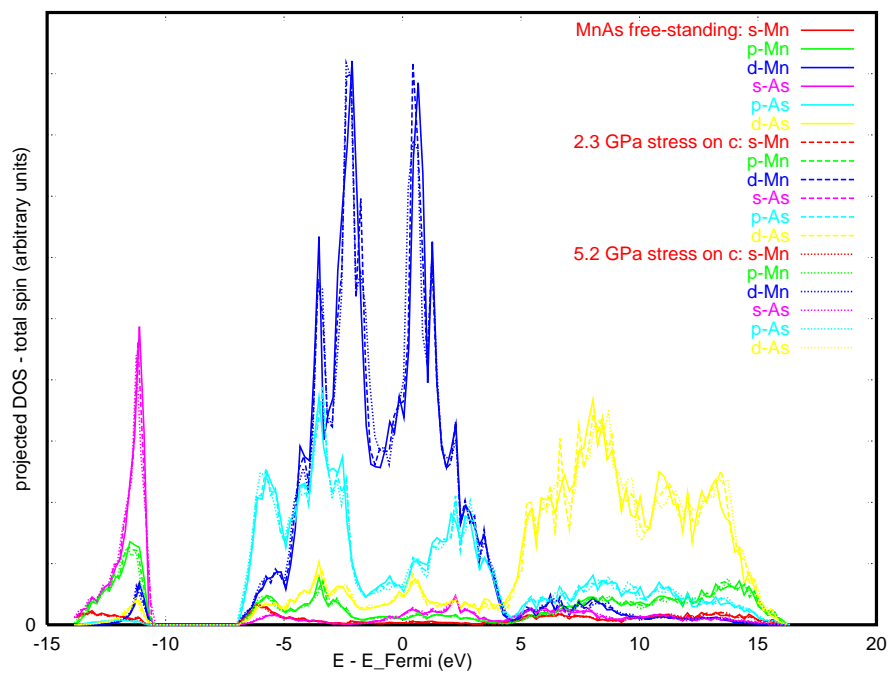
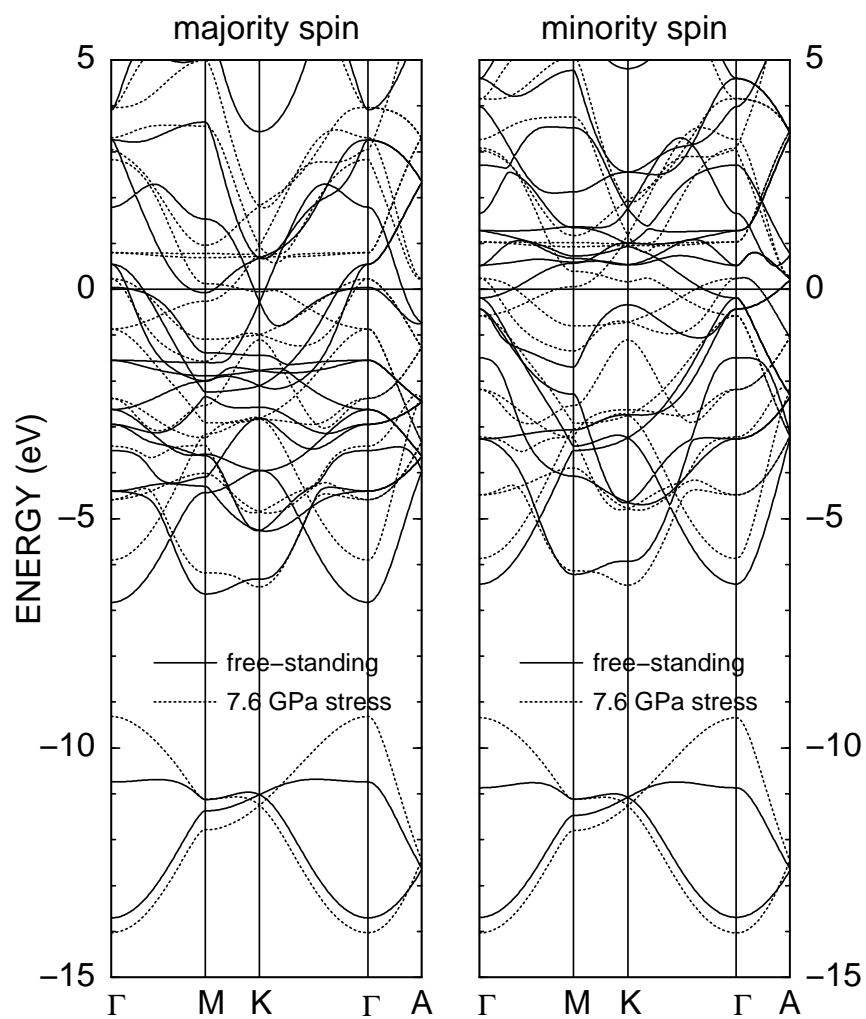


Fig. 5



ELECTRONIC PROPERTIES OF Mn-COMPOUNDS UNDER STRAIN

A. Debernardi,¹ M. Peressi,^{*,1,2} and A. Baldereschi^{1,2,3}

(1) Istituto Nazionale di Fisica della Materia (INFM),
Research Unit of Trieste, via Beirut 4/2, I-34014 Trieste, Italy

(2) Department of Theoretical Physics, University of Trieste,
Strada Costiera 11, I-34014 Trieste, Italy

(3) Ecole Polytechnique Fédérale de Lausanne,
PHB-Ecublens, CH-1015 Lausanne, Switzerland

Abstract

We study the physical properties of MnAs under strain by using accurate first-principles pseudopotential calculations. Our results provide new insight on the physics of strained multilayer that are grown epitaxially on different lattice mismatched substrates and which are presently of interest for spintronic applications. We compute the strain dependence of the structural parameters, electronic bands, density of states and magnetization. In the region of strain/stress that is easily directly accessible to measurements, the effects on these physical quantities are linear. We also address the case of uniaxial stress inducing sizeable and strongly non linear effects on electronic and magnetic properties.

Keywords: MnAs, strain, pseudopotential, magnetic properties, electronic properties, epitaxy

PACS: 71., 71.15.Hx, 71.15.Mb, 71.20.-b, 75.50.-y

1. Introduction

The recent discovery of giant magneto-resistance has driven increasing interest to the study of magnetic materials. The main target is the design

^{0*} Corresponding Author: Tel. +39 040 2240242; Fax. +39 040 224601; E-mail: peressi@ts.infn.it

and the realization of new devices with materials whose magnetic properties could be tailored in accordance to the needs of electronic industry. Within the solid state community is rapidly becoming popular the word "spintronic" to denote electronic-like heterostructures where the relevant physical quantity is the spin of the carriers and its interactions with external magnetic fields rather than the charge of holes and electrons and the associated electronic properties. In this context the most promising materials are Mn compounds.

Although they naturally occur in the hexagonal structure whose symmetry is completely different with respect to the zincblende structure of conventional semiconductors, high-quality epitaxial Mn compounds can be grown on many semiconductor substrates, different for composition and orientation. Realistic cases include the growth on (111)-As-terminated GaAs or (111)Si [1, 2] where the MnAs c -axis is parallel to the (111) zincblende substrate axis, and on (001) GaAs or Si, with two possible different orientations (usually referred as type-A and type-B) of the MnAs c -axis with respect to the zig-zag anion-cation bond chain underlying the substrate surface. A recent experiment [3] has proved the possibility of growing ordered films (heterostructures) of MnAs on ZnSe. The presence of a ZnSe buffer layer exclusively stabilizes a particular phase (type-B) of MnAs; at variance, the coexistence of different phases in the magnetic epitaxial layers is experimentally observed on GaAs substrates [1].

Due to the lattice mismatch with the substrate, which is different according to its composition and orientation, we expect the Mn-compound epilayers to grow in different kind of strained structures, some of them with considerable deformation with respect to the original free-standing structure, and in general of reduced symmetry.

After a description of the structural, electronic and magnetic properties of MnAs in the free-standing hexagonal and zincblende structures, in this paper we address in particular the effects on these properties induced by a uniaxial stress along the c -axis of the hexagonal structure.

2. Computational details

Our calculations are performed within the spin-polarized density functional theory using ab-initio pseudopotentials and plane-wave formulation. For the exchange and correlation energy we use the generalized gradient approximation (GGA) with the Perdew-Wang parameterization [4], that has been shown to provide a good description of the metallic bond. From the comparative tests that we have performed using the local density approximation (LDA) with the Perdew-Zunger parametrization of the exchange and correla-

tion functional [5], we found that GGA slightly improves the agreement of our results with respect to the available experimental data (see Tab. 1). We have generated separable pseudopotentials in the Kleinman-Bylander form [6]: the As pseudopotential has been generated according to the Martins-Troullier technique [7], while the Mn pseudopotential according to the Vanderbilt method [8] which allows to have reliable results with a reasonable size of the plane-wave basis set (corresponding in the present case to a kinetic energy cutoff of 30 Ry). Reciprocal space integration in the Brillouin zone is performed using special k-point techniques [9, 10]. A particular care in the choice of the sampling k-point set must be reserved to the system studied: at zero stress (for the free-standing hexagonal structure) we use a $(12 \times 12 \times 8)$ Monkhorst-Pack [10] grid that corresponds to 336 k-points in the irreducible wedge of the first Brillouin zone, and ensures an accurate convergence of all the electronic properties studied. For the strained structures this set is modified accordingly. The integration over the points of the Brillouin zone are performed with smearing techniques [11] using a Gaussian broadening of 0.02 Ry.

Deformations can be either introduced by constraining the structures in some directions and allowing them to relax in the others (i.e., fixing some components of the strain tensor ϵ_{ij} , as it is the case for epitaxial structures that must accommodate the lattice mismatch with the substrate), or by applying a stress σ_{ij} (external force). We focus here on the last case, *simulating the application of a uniaxial stress along the c axis of the hexagonal structure*, here referred to as the z direction. The correspondent equilibrium lattice structures must have *vanishing stress* along the other directions, i.e. $\sigma_{zz} \neq 0$ and $\sigma_{xx} = \sigma_{yy} = 0$. In practice in the numerical experiments we consider several structures with different strain tensors ϵ_{ij} , with $\epsilon_{xx} = \epsilon_{yy} \neq \epsilon_{zz}$, and we compute the stress tensor σ_{ij} according to the formalism introduced by Nielsen and Martin. [12, 13] The structures can be considered optimized if the residual stress in the xy plane is within $\approx 1\text{kBar}$. We point out that in general this condition is *not* equivalent to the one of volume conservation, i.e. zero-trace strain tensor, and requires a larger computational effort.

3. Results

3.1 Free-standing unstrained structures

In normal free-standing conditions MnAs is a ferromagnetic metal with the NiAs structure, i.e. hexagonal lattice with four atoms in the unit cell, which is described by the parameters a (corner of the hexagon) and c (Fig. 1). The zincblende structure is experimentally observed only for the related alloy

$\text{Ga}_{1-x}\text{Mn}_x\text{As}$ with the extreme diluted concentration of Mn atoms, $x < 0.07$. We will address here also the study of this structure, for a comparison with the hexagonal one. In Tab. 1 we summarize the results for the structural and magnetic properties obtained with our pseudopotentials with GGA, together with those obtained within LDA, and also by other authors using full-potential linearized augmented plane-wave techniques (FLAPW) [14]. The comparison with the available experimental data completes the Table.

Comparing zincblende and hexagonal MnAs, we found that the last one is more dense and more stable (by ~ 0.7 eV); the increase in the atomic distance in the zincblende structure is accompanied by an increase in the total magnetization M_{tot} , which goes from $2.80 \mu_B$ to $3.84 \mu_B$, to be compared with the limiting value of $4 \mu_B$ per MnAs pair for atoms at infinite distance. We compute both the total and the absolute magnetization, $M_{tot} = \frac{1}{\Omega_{cell}} \int (\rho^\uparrow(\mathbf{r}) - \rho^\downarrow(\mathbf{r})) d\mathbf{r}$ and $M_{abs} = \frac{1}{\Omega_{cell}} \int |\rho^\uparrow(\mathbf{r}) - \rho^\downarrow(\mathbf{r})| d\mathbf{r}$.

The two structures are very different as far as the electronic properties is concerned: at variance with the hexagonal phase, the zincblende MnAs is half-metallic, as we show in Fig. 2. From the density of states (DOS) for the majority and minority spin projected onto the different atomic states (not shown here) it is evident the atomic origin (d states of Mn) of the flat bands in the two spin orientations. Our results are in agreement with some obtained from previous pseudopotential calculations. [15]

3.2 Strained structures for applied uniaxial stress

The uniaxial stress along the c axis does not cause any reduction of the symmetry of the structure, which remains hexagonal but with a c/a ratio different from the free-standing one. For uniaxial stresses up to about 5.2 GPa the effects on the structural parameters, electronic structure and magnetic properties are almost linear. For the electronic structure we report the bands for the unstrained and for one strained configuration (Fig. 3, solid and dashed lines), and the total DOS projected onto the different atomic states for the same configurations and for a third one with intermediate strain configuration (Fig. 4). No dramatic changes are observed, only a progressively filling of the DOS around the Fermi energy. The total magnetization reduces linearly with the stress from $2.80 \mu_B$ to $2.65 \mu_B$.

Sizeable changes occur instead for higher uniaxial stress. At about 7.6 GPa the effect of the applied stress on the structural properties is no longer linear: it can be seen in terms of induced strain, or volume change (which amounts to -10%), or reduction of c/a ratio (of about -20% , thus corresponding to a strong cell deformation). Also the effects on the electronic and magnetic properties are important. The band structure (Fig. 5) looks quite

different from the free-standing and from the low-stress region: the bands originating from the d -states of Mn approach the Fermi level, going towards higher energy for the majority spin, and towards lower energy for the minority spin. The net effect is a dramatic reduction of the magnetization, which goes to $0.26 \mu_B$. Although further investigation is needed to better understand the microscopic origin of such effect, our preliminary results seem to indicate that the magnetization reduction is related not simply to a sizeable compression, but, more important, to a strong deformation of the structure.

4. Summary

We calculate the variation of the structural parameters, electronic bands, density of states and magnetization of MnAs under the application of a uniaxial stress along the c axis of the hexagonal structure. We found a region of strain/stress where the effects are linear and rather small, but also a region of sizeable and strongly non linear effects on electronic and magnetic properties.

5. Acknowledgments

Calculations in this work have been done using the PWSCF package [16]. We acknowledge the Istituto Nazionale di Fisica della Materia for the “Iniziativa Trasversale di Calcolo Parallelo”. We acknowledge D. Vanderbilt to have kindly provided us the latest version of his pseudopotential code.

References

- [1] Y. Morishita, K. Iida, J. Abe, K. Sato, Jap. Journ. Appl. Phys. Part 2-Letters, **36** (1997) L1100; M. Tanaka, Physica E **2** (1998) 372; V.H. Etgens, M. Eddrief, D. Demaille, Y.L. Zheng, A. Ouerghi, J. Cryst. Growth **240** (2002) 64, and references therein.
- [2] A. M. Nazmul, A.G. Banskchikov, H. Shimizu, and M. Tanaka, J. Cryst. Growth **227-228** (2002) 874.
- [3] J.J. Berry, S.H. Chun, K.C. Ku, N. Samarth, I. Malajovich, and D.D. Awschalom, Appl. Phys. Lett. **77** (2000) 3812.
- [4] J. P. Perdew and Y. Wang, Phys. Rev. B **45** (1992) 13 224

- [5] J. Perdew and A. Zunger, Phys. Rev. B **23** (1981) 5048.
- [6] D. M. Bylander and L. Kleinman, Phys. Rev. Lett. **52** (1995) 14 566.
- [7] N. Troullier and J. L. Martins, Phys. Rev. B **43** (1991) 1993.
- [8] D. Vanderbilt, Phys. Rev. Lett. **32** (1985) 8412.
- [9] A. Baldereschi, Phys. Rev. B **7** (1973) 5212; D.J. Chadi and M.L. Cohen, Phys. Rev. B **8** (1973) 5747; D.J. Chadi, Phys. Rev. B **16** (1977) 1746.
- [10] H.J. Monkhorst and J.D. Pack, Phys. Rev. B **13** (1976) 5188.
- [11] N. Marzari, D. Vanderbilt, and M. C. Payne Phys. Rev. Lett. **79** (1997) 3296; M. Methfessel and A. T. Paxton, Phys. Rev. B **40** (1998) 3616.
- [12] O. H. Nielsen and R. M. Martin, Phys. Rev. Lett. **50** (1983) 697.
- [13] O. H. Nielsen and R. M. Martin, Phys. Rev. B **32** (1985) 3780.
- [14] A. Continenza, S. Picozzi, W. T. Geng, Y. J. Zhao, and A. J. Freeman, Phys. Rev. B **64** (2001) 085204.
- [15] S. Sanvito and N.A. Hill, Phys. Rev. B **62** (2000) 15553.
- [16] S. Baroni, A. Dal Corso, S. de Gironcoli, and P. Giannozzi, <http://www.sissa.it/cm/PWcodes/>

Table 1

| | crystal str. | E_{xc} | a_L (\AA) | c/a | M_{tot} (μ_B) | M_{abs} (μ_B) |
|--------------------|--------------|----------|---------------------------|-------|--------------------------|--------------------------|
| Pseudo | HEX | LSDA | 3.51 | 1.49 | 2.15 | 2.39 |
| Pseudo | HEX | GGA | 3.64 | 1.50 | 2.80 | 3.13 |
| FLAPW ^a | HEX | LSDA | 3.487 | 1.49 | 1.91 | - |
| FLAPW ^a | HEX | GGA | 3.704 | 1.49 | 3.15 | - |
| Exp. | HEX | | 3.7 | 1.54 | 3.4 | - |
| FLAPW ^a | FCC | GGA | 5.643 | - | 3.83 | - |
| Pseudo | FCC | GGA | 5.69 | - | 3.84 | 4.24 |

^a from Ref. [14]

Table 1: Structural parameters and magnetization for MnAs in the FCC and HEX phases compared with other calculations and with available experiments. The pseudopotential results, both with LDA and GGA, are those obtained in the present work.

Figure 1: The NiAs structure.

Figure 2: Majority and minority bands for the half-metallic zincblende MnAs. The energy zero is set to the Fermi energy.

Figure 3: Majority and minority bands for the ferromagnetic MnAs in the unstrained structure and in the structure corresponding to an applied uniaxial stress on c of 5.2 GPa. The energy zero is set to the Fermi energy.

Figure 4: Total density of states projected onto the different atomic states for the unstrained hexagonal MnAs, and for two different strain conditions corresponding to an applied uniaxial stress on c respectively of 2.6 GPa and 5.2 GPa.

Figure 5: Majority and minority bands for the ferromagnetic MnAs in the unstrained structure and in the structure corresponding to an applied uniaxial stress on c of 7.6 GPa. The zero is arbitrary set to the Fermi energy.